The peroxin Pex14p is the key component for coordinated autophagic degradation of mammalian peroxisomes by direct binding to LC3-II

蒋, 李

https://doi.org/10.15017/1485058

出版情報：九州大学, 2014, 博士（理学）, 課程博士
バージョン：
権利関係：全文ファイル公表済

ABSTRACT

Pexophagy can be experimentally induced in mammalian cells by removing the culture serum. Pex14p, a peroxisomal membrane protein essential for matrix protein import in docking of soluble cargo-receptor Pex5p, is involved in the mammalian autophagic degradation of peroxisomes and interacts with the lipidated form of LC3, termed LC3-II, an essential factor for autophagosome formation, under the starvation condition in CHO-K1 cells. However, molecular mechanisms underlying the Pex14p-LC3-II interaction remain largely unknown. To verify whether Pex14p directly binds LC3-II, I reconstituted an *in vitro* conjugation system for synthesis of LC3-II with recombinant human Atg7, Atg3, and CHO-K1 LC3 mutant harboring the C-terminal Gly exposed, in the presence of ATP and phosphotidylethanolamine (PE)-containing liposomes. I show here that Pex14p directly interacts with LC3-II via the transmembrane domain of Pex14p. Pex5p competitively inhibits this interaction, implying that Pex14p preferentially binds to Pex5p under the nutrient-rich condition. Moreover, a Pex5p mutant defective in PTS1-protein import loses its affinity for Pex14p under the condition of nutrient deprivation, thereby more likely explaining why Pex14p prefers to interact with LC3-II under the starvation condition *in vivo*. I also show that another autophagy factor NBR1 is involved in the peroxisomal degradation and interacts with Pex14p and LC3 under the starvation condition. Together, these results suggest that Pex14p is a unique factor that functions in the dual processes in peroxisomal biogenesis and degradation with the coordination of Pex5p in response to the environmental changes.

Abbreviations:
Atg, autophagy-related genes;
BSA, bovine serum albumin;
CHO, Chinese hamster ovary;
DOPC, 1-dioleoyl-2-oleoyl-phosphatidylcholine ;
DOPE, dioleoyl-phosphatidylethanolamine;
EGFP, enhanced green fluorescent protein;
GST, glutathione S-transferase;
LC3, human microtubule-associated protein I light chain 3;
LC3-I, soluble unmodified form of LC3;
LC3-II, LC3-phospholipid conjugate;
LRS, LC3-recognition sequence;
PBS, phosphate-buffered saline;
PE, phosphatidylethanolamine;
PNS, Post-nuclear supernatant;
PTS1, peroxisome targeting signal type I;
siRNA, small interfering RNA.

INTRODUCTION

Cellular components and organelles in eukaryotic cells are reorganized constitutively to maintain cellular activities, which is highly regulated by various molecular mechanisms of biogenesis and degradation. Autophagy, a catabolic process is involved in the degradation of cellular components and organelles in lysosome. Autophagy is generally thought to be a bulk degradation system to remove cytosolic toxic substrates, to get amino acids for biosynthesis of proteins responding to nutrient starvation or to be protected against infection or stress to maintain cell survival [1-3].

Biochemical and morphological studies revealed the selective peroxisomal degradation by the autophagic mechanism, referred as 'Pexophagy', in several methylotrophic yeasts. In methylotrophic yeast, *Pichia pastoris*, peroxisomes are induced in both number and volume, when cells were grown in the medium containing methanol as a carbon source. After changing the medium containing methanol to glucose or ethanol, the proliferated peroxisomes are rapidly and selectively degraded. There are two processes for selective peroxisomal degradation: macropexophagy and micropexophagy. Macropexophagy is that peroxisomes are selective sequestered individually within a double-membrane structure, autophagosome, which is then fused with vacuoles for degradation [4].

Many autophagy-related genes (Atg) have been identified as essential proteins for autophagic machinery. Atg8, as an essential protein required for formation of autophagosomal membrane, is essential for pexophagy [5]. Atg36 identified in *Saccharomyces cerevisiae* is recruited to peroxisomes through binding to Pex3p, the targeting receptor of peroxisomal membrane proteins [6], and then delivers peroxisomes to the preautophagosomal structure by binding Atg8 [7] under pexophagy condition. In *P. pastoris*, Atg30 is involved in peroxisome recognition for pexophagy by interacting with both Atg8 [8] and peroxisomal proteins (Pex14p and Pex3p) [9]. The two peroxins were also identified as targets for initiation of pexophagy in *Hansenula polymorpha*. Pex3p is rapidly degraded before peroxisomal degradation [10-12], while Pex14p, as a peroxisomal membrane peroxin essential for

matrix protein import [13], is also required for macropexophagy [14, 15].

In mammal, specific peroxisomal degradation by autophagic machinery is observed in rodent liver. When mice are fed with peroxisomal proliferators such as clofibrate, the number and volume of peroxisomes increase in liver cells. After withdrawal of the agents, the proliferated peroxisomes are then decreased via autophagic degradation [16]. There are also different types of pexophagies have been observed in mammalian cells. And the peroxins Pex3p and Pex14p function not only in pexophagy in yeast, but also in mammalian cells. Our recent study reveals a novel condition for Pex3p-mediated pexophagy [17], similar to the effect of NBR1 (neighbor of BRCA1 gene 1) over-expression in mammalian cells [18]. It has been reported that Pex14p is involved in the degradation of peroxisomes triggered experimentally by switching the nutrient-rich medium to nutrient-starved medium in cultured cells, which interacts with LC3-II, one of the mammalian homologues of Atg8, via microtubules under the nutrient-starved condition [19]. LC3-II is the membrane-bound form of LC3-I, and is essential for autophagosome formation and remains on autophagosomal membrane [20, 21]. The selectivity of autophagy can be mediated by the binding of organelle receptors to LC3. Many LC3-binding proteins contain a W/YXXL motif [22, 23] or alternatively termed LC3-recognition sequence (LRS) [24, 25]. However, Pex14p does not contain LRS and little is known about how Pex14p interacts with LC3-II.

Pex5p, the peroxisome targeting signal 1(PTS1) [26] receptor, shuttles between the cytoplasm and peroxisomes. Pex5p transports peroxisomal matrix proteins synthesized on cytosolic ribosomes to the organelle matrix through the N-terminal of Pex14p involved in a multi-subunit protein complex as the first step [27-29]. However, Pex14p efficiently interacts with LC3-II under the starvation condition, whilst it binds to Pex5p under the normal condition [19].

In this study, to elucidate whether Pex14p directly binds to LC3-II, *in vitro* binding system using cell-free synthesized LC3-II and recombinant Pex14 was established. I showed here the direct binding of Pex14p to LC3-II and defined the binding region of LC3-II in Pex14p. And I also investigated how Pex14p interacts with LC3-II under the starvation condition and proposed that Pex5p is the cytosolic factor for the

regulation of their interaction.

EXPERIMENTAL PROCEDURES

Cell culture

CHO-K1 cells and CHO cell mutants including *pex14* ZP161 [30]. *pex5* ZPEG101 [31] and *pex5* ZP139 [32] were cultured in Ham's F-12 medium supplemented with 10% fetal bovine serum under 5% CO_2. For nutrient-starved condition, cells were washed with Hank's solution and incubated in the same solution at 37°C.

Antibodies

The antibodies used were rabbit antibodies to Atg3 (Cell Signaling Technology), Pex5p [33], Pex14pC [34] and acyl-CoA oxidase (AOx) [35], mouse monoclonal antibodies to NBR1 (Abnova), tubulin α (Abcam) and His_6 tag (Biodynamics Laboratory), goat antibody to lactate dehydrogenase (LDH) (Lockland), and guinea pig antibody to Pex14pN [36]. Rabbit polyclonal anti-LC3 antibody raised against a synthetic peptide corresponding to the N-terminal 19 amino acids of Chinese hamster LC3 [19] was also used.

Preparation of liposomes

Synthetic phospholipids, 1-dioleoyl-2-oleoyl-phosphatidylcholine (DOPC) and dioleoyl-phosphatidylethanolamine (DOPE), were purchased from Avanti Polar Lipids (Alabaster). To prepare dried lipid films, the chloroform was evaporated with nitrogen gas. The resultant dried lipid films were hydrated to a final concentration of 1 mM phospholipids in a buffer containing 25 mM Tris-HCl (pH 7.5), 0.15 M NaCl, 3 mM KCl, vortexed vigorously at room temperature, and sonicated at 4°C for 5 min. After centrifugation at 20,000 × *g* for 20 min, the supernatant was used as small unilamellar liposomes.

Plasmids

Plasmids each of pGEX-4T-1 inserted with cDNA encoding human Atg7 and human Atg3, respectively, were provided by Dr. I. Tanida [21]. Chinese hamster LC3B

cDNA was as described [19]. LC3 mutant exposing C-terminal Gly was constructed in plasmid pGEX-6P-3 by inserting a stop codon after the codon for Gly 373. *BamH1-EcoR1* fragments of LC3B mutant were amplified with *BamH1*-LC3B-sense primer [19] and the designed LC3B-G-stopcodon-*EcoR1*-antisense primer (5'-CCGGGAATTCTTACCCGAACGTCT-3') using pGEX-6p-3-LC3B as a template. They were then subcloned into *BamH1* and *EcoR1* sites of pGEX-6p-3 vector. The sequence for the mutation was confirmed by DNA sequencing. cDNAs coding for glutathione S-transferase (GST), GST-Pex14p, and mutant GST-Pex14p in pGEX6P-2 were provided as described [29]. cDNAs coding for GST-catalase was provided by Dr. K. Okumoto [37]. pEGFP-LC3 coding for enhanced green fluorescent protein fused to LC3 was as described [17]. cDNAs coding for His_6-tagged Pex14p (His-Pex14p) [29] and Pex5pL (His-Pex5pL) [33] were also used.

Purification of recombinant proteins

GST-fused proteins were expressed in *Escherichia coli* and affinity-purified using glutathione-linked Sepharose 4B as described [38]. PreScission protease or thrombin was used for cleaving GST-fused proteins according to the manufacturer's protocol (Amersham Biosciences). His-Pex14p and His-Pex5pL were expressed in *E. coli* and purified using nickel-nitrilotriacetic acid-agarose (Ni-NTA) (QIAGEN).

***In vitro* conjugation reaction for synthesis of LC3-II**

Reaction mixture each containing liposomes (300 μM lipids), purified hAtg7, hAtg3, LC3 harboring the C-terminal glycine residue (0.1 μM each), 1 mM ATP, and 1 mM $MgCl_2$ were incubated at 30 °C for 1 h in reconstitution buffer contains 100 mM NaCl, 0.2 mM dithiothreitol, and 50 mM Tris-HCl, pH 8.0. The reaction can be terminated by adding 50% volume of 2 × SDS-PAGE sample buffer for SDS-PAGE and western blotting. Addition of NP-40 to the reaction mixture at a final concentration of 1% was also used for further binding assays.

DNA transfection

DNA transfection into CHO-K1 cells was performed with Lipofectamine reagent (Invitrogen) as described [39].

***In vitro* binding assays**

GST-fused Pex14p and its various deletion mutants were purified, immobilized to GSH conjugated Sepharose 4B, and incubated with the mixture of LC3-II conjugation system at 4°C for 2 h in the presence of 1% NP-40. GST beads were washed 3 times with reconstitution buffer. Samples were denatured in SDS sample buffer and analyzed by SDS-PAGE and immunoblotting with anti-LC3 antibody.

The organelle fraction was prepared from *pex14* ZP161 cells cultured under the starvation condition and incubated with anti-LC3 antibody for 1 h on ice. Protein A-Sepharose was added to immobilize LC3 bound to anti-LC3 antibody by incubating at 4℃ for 1 h. LC3-bound Protein-A Sepharose was washed twice with 1% NP-40 lysis buffer (1% NP-40, 150 mM NaCl, 50 mM Tris-HCl, pH 8.0). For binding assay, recombinant His-Pex14p was added to the immobilized LC3 together with cell lysate prepared from CHO-K1 or *pex5* ZPEG101 cells. The mixture was incubated at 4℃ for 2 h and the Protein A-Sepharose pellet was washed 3 times with lysis buffer and treated with SDS-PAGE sample buffer at 95℃ for 5 min, His-Pex14p bound to LC3 was analyzed by SDS-PAGE and western blotting.

Immunoblot and immunoprecipitation

For immunoblot, cells were washed twice with phosphate-buffered saline, homogenized in 0.25 M sucrose, 5 mM Hepes–KOH, pH 7.4, and 1 mM EGTA, containing protease inhibitor cocktail and 1 mM phenylmethylsulfonyl fluoride. Post-nuclear supernatant (PNS) fraction of cells was prepared by centrifuging the cell-homogenates at 800 × *g* for 5 min and subjected for protein quantitation. The samples each contains equal protein amount were separated by SDS-PAGE, and transferred to polyvinyledene difluoride membranes (Bio-Rad). Samples on the membrane were subjected to the detection with primary antibodies, secondary

antibodies conjugated to horseradish peroxidase (GE Healthcare, Japan), and ECL reagent (GE Healthcare, Japan). For immunoprecipitation, cytosol and organelle fractions were prepared by centrifuging the PNS fraction at 100,000 × *g* for 30 min. The organelle fraction was solubilized in 50 mM Tris-HCl, pH 7.4, 1% NP-40, and 150 mM NaCl. The cytosol and solubilized membrane fractions were incubated with anti-LC3 antibody on ice for 2 h. The antigen-antibody complexes were recovered with Protein A-Sepharose beads (GE Healthcare, Japan) and were analyzed by SDS-PAGE and immunoblotting. For immunoprecipitation assay using anti-NBR1 antibody, cells were directly lysed with lysis buffer and incubated with agarose beads coupled with anti-NBR1 antibody on ice for 2 h. The immunoprecipitation complexes were analyzed by SDS-PAGE and immunoblotting.

Protein delivery

Proteins were induced into CHO-K1 cells using BioPORTER (Genlantis) as in the manual of manufacturer.

RNA interference

For small interfering (siRNA)-mediated knockdown of NBR1, cells were transfected with 100 nM of the targeting siRNA using Lipofectamine 2000 (Invitrogen) for 48 h.

Immunofluorescence microscopy

Cells expressing with cDNA encoding enhanced green fluorescent protein (EGFP)-fused LC3 were grown on a cover-glass under normal culture condition or nutrient-starved condition. Cells were permeabilized with 50 μg/ml of digitonin, fixed with 4% paraformaldehyde (PFA), and blocked over night at 4°C with 1% bovine serum albumin (BSA) in phosphate-buffered saline (PBS). Cells were stained with antibody to Pex14p and secondary antibody of Alexa 568 goat anti-guinea pig IgG. Confocal images were obtained by a confocal laser microscope LSM510 (Carl-Zeiss) with a 100 × oil lens.

RESULTS

Pex14p is important for autophagic degradation of peroxisomes by binding to LC3 under the starvation condition

Previous report showed the degradation of peroxisomes in response to the nutrient-starvation [19]. Under the starvation condition, LC3-II was co-immunoprecipitated with Pex14p, and with concomitant reduction of the binding of Pex5p to Pex14p (Fig. 1A). No matter how significantly high the expression of autophagy marker LC3-II is in CHO-K1 cells starved in Hank's solution, the degradation of peroxisomes become evident only when the cells are re-cultured in a normal medium after the starvation [19] (Fig. 1B, panels e-l). The colocalization of LC3-II-marked peroxisomes with lysosomes was obviously detected in the presence of Chloroquine, an inhibitor of autophagy, after the re-culture (Fig. 1B, panels m-p). These results confirmed the previous demonstration that peroxisomes are degraded by autophagy system in the culture medium after the starvation treatment, where Pex14p plays a key role at the initial step in binding to LC3-II under the starvation condition.

LC3-II is synthesized *in vitro*

LC3 is one of mammalian homologue of yeast Atg8, which is a ubiquitin-like protein and plays an essential role in autophagy through its ability to be conjugated to phosphatidylethanolamine (PE) [40-42]. When autophagy is initiated, the cytosolic form of LC3-I is converted to LC3-II through lipidation of C-terminal glycine residue with PE by a ubiquitin-like conjugation system [20]. LC3 is cleaved by Atg4B, an authentic cysteine protease, to expose the C-terminal glycine, resulting in LC3-I. And LC3-I is then activated by Atg7 as E1-substrate in an ATP-dependent manner, transferred to Atg3 as E2-substrate, and finally conjugated to PE [20, 43]. To confirm whether the interaction between Pex14p and LC3 is direct, a cell-free system was established and used to exclude a possibility that any other factors, if any, co-purified by immunoprecipitation of LC3-II are involved in this interaction.

In order to conjugate LC3 to PE, LC3-I harboring the C-terminal Gly exposed ($LC3_{TFG}$), Atg7, Atg3, and PE-containing liposomes were prepared as minimum reaction units required for *in vitro* lipidation system（Fig. 1A）. In CHO-K1 cells, two isoforms, LC3A and LC3B, were identified in the LC3 family [44]. Previous study showed that LC3B is preferentially expressed and mainly functions as the yeast Atg8 counterpart in CHO-K1 cells [19]. Therefore, CHO-K1 LC3B was used in this study and its C-terminal Gly-exposed mutant termed $LC3_{TFG}$, was constructed. Respectively purified proteins were subjected to SDS-PAGE and staining with by Coomassie Brilliant Blue (Fig. 2A). At first, the E1-substrate intermediate between hAtg7 and $LC3_{TFG}$ was formed. hAtg7 and $LC3_{TFG}$ were mixed and incubated at 30°C for the indicated time period in the presence or absence of ATP (Fig. 2B). Reaction was stopped by addition of SDS-PAGE sample buffer and the reaction mixture was subjected to SDS-PAGE under non-reducing condition. $LC3_{TFG}$ was detected by immunoblotting using anti-LC3 antibody. In the presence of ATP, a band with ~100 kDa apparently corresponding to hAtg7-$LC3_{TFG}$ intermediate formed after 15-min incubation (Fig. 2B, lanes 2-4) and disappeared after 60-min incubation (Fig. 2B, lanes 5-7). The intermediate was not detected in the presence of a reducing reagent, dithiothreitol (DTT), apparently because the intermediate was formed via a thioester bond (Fig. 2B, lane 9). Next, to synthesis an E2-substrate intermediate between hAtg3 and $LC3_{TFG}$, three recombinant proteins including hAtg7, hAtg3 and $LC3_{TFG}$ were incubated at 30°C for 60 min (Fig. 2C). Incubating for longer than 60 min seemed to affect the stability and activity of hAtg7 (Fig. 2B, lanes 5-7). To stop the reaction, an equal volume of SDS-PAGE sample buffer excluding β-mercaptoethanol was added and the mixture was analyzed by SDS-PAGE gel under non-reducing condition. hAtg3-LC3 intermediate was detected by immunoblotting with anti-LC3 antibody and anti-Atg3 antibody. In the presence of ATP, a ~60kDa band corresponding to hAtg3-$LC3_{TFG}$ intermediate was detected (Fig. 2C, lane 3), which was not detectable in the absence of hAtg7 (lane 1) or ATP (lane 2). Since 100% DOPE is not structurally suitable for formation of liposomes [21], I prepared two kinds of DOPE-containing liposomes and investigated their effects on LC3 conjugation. Other

components including hAtg7, hAtg3, $LC3_{TFG}$ and ATP were incubated at 30°C for 60 min with either of DOPE-containing liposomes (70% DOPE and 30%DOPC; 50% DOPE and 50% DOPC). LC3-II formation was observed in both reactions (Fig. 2D). To concentrate the synthesized LC3-II after the reaction, the mixture was centrifuged. LC3-II was mostly harvested in the pellet fraction as expected (Fig. 2E, lane 5). By optimizing the reaction conditions, under which the purified recombinant proteins including hAtg7, hAtg3, and $LC3_{TFG}$ were incubated with PE-containing liposomes, LC3-II was significantly generated after incubation in the presence of ATP (Fig. 2F, lane 2).

Transmembrane domain of Pex14p is essential for LC3-II binding.

Recombinant GST-Pex14p and GST-p62 were verified for binding to LC3-II synthesized by cell-free system. p62 is a well-known substrate for mammalian autophagy and contains an LRS motif [45]. Synthesized LC3-II was pulled down by GST-Pex14p and GST-p62, but not GST used as a negative control (Fig. 3A). These results suggest that Pex14p directly binds to LC3-II. Although I noted that Pex14p binding to LC3-I, *in vivo* studies showed that Pex14p predominantly interacts with LC3-II [19]. Therefore, it is likely that the lipidation of LC3-I to LC3-II is required for activation of peroxisomal degradation via Pex14p.

Pex14p contains three distinct parts, a highly conserved N-terminal region, a typical coiled-coil domain in the middle, and a C-terminal region. Three peroxins, Pex5p, Pex13p, and Pex19p, share the same domain of the N-terminal Pex14p for interaction. The coiled-coil domain of the middle part is reported to be responsible for oligomerization of Pex14p while little is known about the functions of C-terminus [29, 34, 46, 47]. There is no report about LRS in Pex14p, while it is well known in p62. To determine the domains of Pex14p involved in the binding to LC3-II, GST-fused full-length and truncated forms of Pex14p were constructed (Fig. 3B) and expressed in *E.coli*. *In vitro* LC3-II-binding assays by GST-pull down method revealed that the Pex14p N-terminal fragment comprising amino-acid sequence at 21 to 140 interacted with LC3-II, whereas the construct encompassing the sequence at 1 to 106 did not

bind to LC3-II (Fig. 3C). These results suggest that the region encompassing the amino acid residues between 106-140 containing the hydrophobic transmembrane domain (110-138) of Pex14p is essential for binding to LC3-II, implying that Pex14p interacts with LC3-II directly in the peroxisomal membrane.

Pex5p competes with LC3-II in binding to Pex14p

Pex5p is the peroxisome-targeting signal 1 (PTS1) receptor and shuttles between the cytoplasm and peroxisomes. Pex5p binds to Pex14p at the first step of the matrix-protein import process through the N-terminal region of Pex14p [29, 46, 47]. Previous report [19] showed that, under the starvation condition, LC3-II was co-immunoprecipitated with Pex14p, and with concomitant reduction of Pex5p binding to Pex14p (Fig. 1A). To assess whether Pex5p contributes to the regulation of the interaction between Pex14p and LC3-II, cytosolic fraction from *pex5* CHO mutant ZPEG101 cells [31] was examined by a binding assay system using LC3-II purified from the membrane fraction of the starved *pex14* CHO mutant ZP161 cells. Recombinant His-Pex14p was pulled down *in vitro* with the purified LC3-II (Fig. 4A, lane 4). Binding of His-Pex14p to LC3-II was lowered by increasing amount of the cytosolic fraction prepared from CHO-K1 cells, but not by that from *pex5* ZPEG101 cells lacking Pex5p (Fig. 4B). Moreover, to assess whether such inhibition is direct, I examined the effects of recombinant Pex5p addition to the pull-down assay. Pex5p effectively inhibited the binding of His-Pex14p to LC3-II (Fig. 4C). Morphological analysis was also performed using CHO-K1 cells stably expressing EGFP-LC3B. Recombinant His-Pex5pL was introduced into cells using BioPORTER for the delivery. When cells were grown under nutrient-rich condition, EGFP-LC3B was not detected as a punctate structure since LC3 was mainly in cytosolic form (LC3-I) under the nutrient-rich condition (Fig. 4D, panel c). On the contrary, EGFP-LC3B puncta were induced and partly colocalized with peroxisomes under the starvation condition, suggesting that autophagy was initiated and some portion of EGFP-LC3B-II bound to Pex14p (Fig. 4D, panel g). To assess the effect of Pex5p on the localization of EGFP-LC3B at peroxisomes, recombinant His-Pex5pL was

introduced into the cells using BioPORTER. Recombinant His-Pex5pL was effectively delivered into cells (Fig. 4E, lanes 2 and 3) and inhibited the colocalization of EGFP-LC3B with Pex14p (Fig. 4D, panels i to l, Fig. 4F). These results suggest that Pex5p functions as an inhibitory factor for the binding of Pex14p to LC3-II. Moreover, I also examined the impact of Pex5p introduction on peroxisomal degradation activity. Reduced level of Pex14p was detected after starvation and re-cultured in the normal medium (Fig. 4G, lanes 1 and 2) and the decrease was inhibited in the presence of Chloroquine (Fig. 4G, lanes 2 and 3), an autophagy inhibitor, indicating it was an autophagic degradation. Peroxisomal matrix protein as AOx also showed similar results. However, after introduction of His-Pex5pL, LC3-II level was apparently inhibited even under the starvation condition (Fig. 4G, lane 4). Pexophagic activity could not be detected with AOx (Fig. 4G, lanes 4-6). Introduced His-Pex5pL and Pex14p presented distinct degradation after re-culture (Fig. 4G, lanes 4 and 5) while the degradation could not be prevented with Chloroquine (Fig. 4G, lanes 5 and 6). I interpreted these results to mean that introduced Pex5p inhibited pexophagy activity when starved and then re-cultured while some non-selective degradation including some peroxisomal proteins was triggered under such condition.

Import defect caused by starvation initiates peroxisomal degradation

The results described above evidently showed that the transmembrane domain of Pex14p, not Pex5p binding region, is required for LC3-II binding. And Pex5p exerts the adverse effect on the interaction between Pex14p and LC3-II. Taken together, these results suggest that LC3-II does not directly compete with Pex5p in binding to Pex14p. Pex5p transports newly synthesized proteins into peroxisomal matrix by docking to Pex14p on peroxisomal membrane, and then translocates via RING peroxins comprising Pex2p, Pex10, and Pex12p, and shuttles back to the cytosol via Pex1p-Pex6p-Pex26p complexes [27, 33, 37, 48-50]. To examine the relationship on the function of Pex5p, matrix protein import and competitive effect to the Pex14p-LC3-II interaction, I investigated the activity of peroxisomal matrix protein under nutrient-rich and deprivation condition. The effective peroxisomal import was

assessed by colocalization of both PTS1 (Fig. 5A, panels a-c) and PTS2 (Fig. 5A, panels g-i) signals with Pex14p under the normal condition. Under the starvation condition, not only Pex5p (Fig. 5A, panels d-f) but also PTS2 protein thiolase displayed minimal translocation to Pex14p (Fig. 5A, panels j-l), indicating that the import activity was significantly lowered under the starvation condition. ZP139 is a *pex5*-defective CHO cell line, which has a phenotypic deficiency in the import of PTS1 proteins [32]. The mutation in ZP139 cells causes the dysfunction of Pex5p in protein-cargo translocation with the intact Pex14p-binding motifs [32, 50]. Therefore, it is likely that Pex5p is mostly cargo-unloaded in ZP139 cells. Pex14p is co-immunoprecipitated with LC3 under the normal culture condition in ZP139 cells (Fig. 5B, lane 6). Under the starvation condition, the binding of LC3 to Pex14p was highly enhanced (Fig. 5B, lane 8). These results were confirmed by morphological analysis. Colocalization of LC3-II with Pex14p was not evident in CHO-K1 cells (Fig. 5C, panels a-d), whilst their colocalization was clearly discernible in ZP139 cells even under the normal condition (Fig. 5C, panels i-l), consistent with the results of coimmunoprecipitation assay. Cytosolic Pex5p was significantly eliminated under the starvation condition in *pex5* ZP139 cells (Fig. 5B, lane 7). Moreover, prolonged starvation treatment of ZP139 cells enhanced the decrease in the level of Pex5p (Fig. 5E, lower panel). Pex14p was concomitantly reduced upon the elimination of Pex5p after 5 h starvation treatment (Fig. 5E, upper panel). These results imply that dysfunctional Pex5p is to be ultimately eliminated in response to nutrient-starvation in ZP139 cells, thereby accelerating the induction of peroxisome degradation. Therefore, one possibility is that the cargo-loading scale of Pex5p is altered on the culture conditions, which then imposing the influence on its affinity for Pex14p. To address whether less PTS1 cargoes are loaded to Pex5p under the starvation condition than the normal condition, I established a pull-down system using purified GST-fused catalase, a matrix PTS1-like enzyme, and cytosolic fractions each from CHO-K1 cells cultured under the normal and starvation conditions. As expected, less amount of Pex5p was pulled down from the cytosol fraction from the cells cultured under the starvation condition as compared to that from normally cultured cells (Fig. 5G),

suggesting a weak association between Pex5p and catalase under starvation. Collectively, these observations suggest that the down-regulation of matrix protein import into peroxisomes under the starvation condition gives rise to the affinity to LC3-II of Pex14p. I also noticed that the reduction of Pex5p and Pex14p in ZP139 cells under the starvation condition was not autophagy-related since it was not prohibited by autophagy inhibitor, Bafilomycin A1 (Fig. 5F, lanes 3 and 4). There are two degradation systems for peroxisomal proteins involving autophagy and proteasomes depending on various cell-culture conditions [19]. I interpreted that down-regulation of Pex5p in ZP139 cells not only enhanced pexophagy but also triggered other non-selective degradation system after longer starvation treatment.

NBR1 is involved in the selective degradation of peroxisomes triggered by nutrient deprivation

To further verify the pivotal role of Pex14p in peroxisomal degradation, I investigated the relation between Pex14p and NBR1, which is one of the essential factors for pexophagy [17, 18], in the initiation of peroxisomal degradation triggered by starvation treatment. Pex14p was detectable in immunoprecipitate of NBR1 in the lysates of CHO-K1 cells cultured under both normal and starvation conditions (Fig. 6A, lanes 5 and 6). LC3-II was also coimmnoprecipitated with NBR1 using anti-NBR1 antibody, predominantly upon the starvation condition (Fig. 6A, lanes 5 and 6). Moreover, NBR1 was localized to peroxisomes under the starvation condition, as verified by morphological analysis (Fig. 6B). These results strongly suggest that NBR1 is involved in the process of initiation of peroxisome degradation by binding to Pex14p in response to the nutrient deprivation. Recent study showed the knockdown of Pex14p impaired the recruiting of NBR1 to peroxisomes in mammalian cells [18]. Taken together, I conclude that Pex14p is a significant factor involved in recruiting autophagic proteins including NBR1, ultimately leading to the shift from biogenesis to degradation. Furthermore, upon knocking down of NBR1, LC3-II was much less recruited to peroxisomes, suggesting a significant decrease in pexophagy (Fig. 6B and C). The binding between Pex14p and LC3-II was considered as the initiation of

starvation-induced pexophagy [19]. It is equally likely that NBR1 might be an association factor for Pex14p-LC3-II binding.

DISCUSSION

In the present work, the results showed that LC3-II was formed *in vitro* using purified hAtg7, hAtg3, CHO-K1 LC3B mutant exposing the glycine residue at C-terminus, ATP and PE-containing liposomes (Fig. 2, A and F), which were a minimum unit for the reconstitution reaction. E1- and E2-substrate intermediates, LC3-hAtg7 and hAtg3-LC3, respectively, via ATP-dependent thioester bonds were also detected (Fig. 2, B and C). Although LC3-II was successfully synthesized *in vitro*, the efficiency in the conversion of LC3-I to LC3-II remained to be improved. *In vivo*, the conjugation activity of Atg3 is a rate-limiting step and Atg12-Atg5 complex can enhance this activity through direct interaction with Atg3 [20, 43]. Therefore, addition of recombinant Atg12-Atg5 into the conjugation system might augment LC3-II formation. Moreover, the reaction conditions including pH and lipid compositions of liposomes need to be optimized. *In vitro* LC3-II conjugation appears to be much more difficult than Atg8-PE conjugation [20, 43]. It is likely that other factors activate the selective conjugation of LC3-I to PE in mammalian cells.

The dynamic nature of peroxisomes is maintained by organelle biogenesis and degradation. Our current studies revealed the significant role of Pex14p on the molecular mechanism underlying the selective degradation of peroxisomes in mammalian cells, such as macropexophagy in methylotrophic yeast *H. polymorpha* [51]. In autophagy degradation of mitochondria termed mitophagy, similar to Pex14p in pexophagy, mitochondrial outer membrane proteins Bcl2/E1B 19 kDa-interacting protein 3-like protein, BNIP3L/Nix [22] and FUN 14 domain containing 1, FUNDC1 [23] are mammalian mitophagy receptors and interact with LC3 under mitophagy conditions. Unlike Nix or FUNDC1 which was shown to contain a W/YXXL motif [22, 23], I showed in the present work that LC3-II directly bound to the transmembrane domain of Pex14p, and it was competitively inhibited by Pex5p. The N-terminal region encompassing 21-70 amino-acid residues of Pex14p is the binding domain for Pex5p that transports newly synthesized peroxisomal matrix proteins from cytosol to peroxisome matrix [29, 46, 47]. Interestingly, it means that LC3-II and

Pex5p do not directly compete in binding to Pex14p. And actually, cytosolic Pex5p shows no evident change at the preliminary stage of starvation treatment. It is reported that cargo-loaded Pex5p in mammalian cells prefers to bind to Pex14p than to Pex13p, whereas cargo-free Pex5p likely binds to Pex13p [37, 52]. These studies have led to the suggestion that cargo-loaded Pex5p has a greater affinity to Pex14p than cargo-free Pex5p. I assumed that upon starvation, a less amount of cargoes is loaded to Pex5p upon certain modification, leading to less affinity of Pex5p towards Pex14p. As shown in Figure 5G, Pex5p in the cytoplasm of starved cells indeed showed less affinity to catalase, a PTS1-like protein [37]. In the presence of Pex5p with apparently lower transport function, LC3-II interacts with Pex14p even when cells are grown under the normal condition. Furthermore, in ZP139 cells, “unnecessary” Pex5p was eliminated by prolonged starvation treatment and the interaction between Pex14p and LC3-II was observed more effectively. As the amount of dysfunctional Pex5p tapered in cytoplasm, the expression level of Pex14p was decreased after long-time amino acid deprivation, apparently leading to the peroxisome degradation. This conditional selective degradation is apparent even when cells are placed in a medium that would normally require peroxisome biogenesis for cell growth. Our finding that incapacitating the function of Pex5p in matrix protein import is a prerequisite for the initiation of peroxisomal degradation suggests a difference between the yeast and mammalian systems.

The topology of Pex14p is not completely defined. It is commonly thought that C-terminal region of Pex14p is exposed to the cytosol and N-terminal part is reported to face to the cytosol by epitope-tagging [53]. But, how the transmembrane domain is embedded into the peroxisomal membrane remains unsolved. Pex14p forms a homo-oligomer via the coiled-coil domain, giving rise to a high molecular mass complex for Pex5p docking. Disassembly of Pex14p homo-oligomer upon the cell-starvation condition may provide a scaffold in the transmembrane domain for LC3-II binding. Recently, NBR1 is shown to be required for the turnover of peroxisomes [18]. NBR1 induces peroxisome clustering and the clustered peroxisomes are degraded by an autophagic pathway [18]. However, it is still unclear

what is the target for NBR1 on peroxisomes. I found that NBR1 targets to peroxisomes under the starvation condition and that it interacts with Pex14p as well as p62, which is another crucial autophagy factor, consistent with previous reports that NBR1 works cooperatively with p62 [54]. p62 can recruit LC3 via its LRS for autophagic degradation of p62-positive inclusion body [24]. Interestingly, NBR1 showed a positive effect on the binding between Pex14p and LC3 since the decreased expressing level of NBR1 led to less LC3-II recruited to peroxisomes. Therefore, I propose that by sensing the nutrient condition, either p62 or NBR1 is initially targeted to peroxisomes by binding to Pex14p, thereby conferring a conformational change of Pex14p homo-oligomer. The disassembly of Pex14p gives rise to the exposure of membrane interaction domain, where LC3-II can anchor, then inducing autophagic sequestration of peroxisomes. This hypothesis implies a dual functional role of Pex14p and explains how the conversion of peroxisomes from biogenesis to degradation takes place.

Autophagy is involved in cell survival, cell death, normal development, negative control of cell growth, longevity, clearance of toxic aggregate-prone proteins, and cell surface receptor trafficking [55]. Pexophagy, the selective degradation of peroxisomes via autophagy machinery, also contributes to the quantitative regulation of peroxisomes and homeostasis in the metabolism of numerous substrates including lipid [56]. Despite the distinct importance of pexophagy in the physiology of higher eukaryotes, the molecular mechanisms and functions of pexophagy in these organisms need to be defined more in details. The findings in the present work would open a way to addressing these issues.

REFERENCES

1. Klionsky, D.J. & Ohsumi, Y. (1999) Vacuolar import of proteins and organelles from the cytoplasm. *Annu. Rev. Cell Dev. Biol.* **15**, 1-32.

2. Mijaljica, D., Prescott, M., Klionsky, D.J. & Devenish, R.J. (2007) Autophagy and vacuole homeostasis: a case for self degradation? *Autophagy* **3**, 417-421.

3. Mizushima, N. & Klionsky, D.J. (2007) Protein turnover via autophagy: implications for metabolism. *Annu. Rev. Nutr.* **27**, 19-40.

4. Xie, Z. & Klionsky, D.J. (2007) Autophagosome formation: core machinery and adaptations. *Nat. Cell Biol.* **9**, 1102-1109.

5. Monastyrska, I., van der Heide, M., Krikken, A.M., Kiel, J.A.K.W., van der Klei, I.J. & Veenhuis, M. (2005) Atg8 is essential for macropexophagy in *Hansenula polymorpha*. *Traffic* **6**, 66-74.

6. Baerends, R.J.S., Rasmussen, S.W., HIlbrands, R.E., van der Heide, M., Faber, K.N., Reuvekamp, P.T., Kiel, J.A.K.W., Cregg, J.M., van der Klei, I.J. & Veenhuis, M. (1996) The *Hansenula polymorpha* PER9 gene encodes a peroxisomal membrane protein essential for peroxisome assembly and integrity. *J. Biol. Chem.* **271**, 8887-8894.

7. Motley, A.M., Nuttall, J.M. & Hettema, E.H. (2012) Pex3-anchored Atg36 tags peroxisomes for degradation in *Saccharomyces cerevisiae*. *EMBO J.* **31**, 2852-2868.

8. Farré, J.-C., Burkenroad A., Burnett, S.F. & Subramani, S. (2013) Phosphorylation of mitophagy and pexophagy receptors coordinates their interaction with Atg8 and Atg11. *EMBO Rep.* **14**, 441-449.

9. Farré, J.-C., Manjithaya, R., Mathewson, R.D. & Subramani, S. (2008) PpAtg30 tags peroxisomes for turnover by selective autophagy. *Dev. Cell*. **14**, 365-376.

10. Bellu , A.R., Salomons, F.A., Kiel, J.A.K.W., Veenhuis, M. & van der Klei, I.J. (2002) Removal of Pex3p is an important initial stage in selective peroxisome degradation in *Hansenula polymorpha*. *J. Biol. Chem.* **277**, 42875-42880.

11. Haan, G.J., Faber, K.N., Baerends, R.J.S., Koek, A., Krikken, A., Kiel, J.A.K.W., I.J., v.d.K. & Veenhuis, M. (2002) *Hansenula polymorpha* Pex3p is a peripheral component of the peroxisomal membrane. *J. Biol. Chem.* **277**, 26609-26617.

12. Leão, A.N. & Kiel, J.A.K.W. (2003) Peroxisome homeostasis in *Hansenula polymorpha*. *FEMS Yeast Res.* **4**, 131-139.

13. Komori, M., Rasmussen, S.W., Kiel, J.A., Baerends, R.J., Cregg, J.M., van der Klei, I.J. & Veenhuis, M. (1997) The *Hansenula polymorpha* PEX14 gene encodes a novel peroxisomal membrane protein essential for peroxisome biogenesis. *EMBO J.* **16**, 44-53.

14. Bellu, A.R., Komori, M., van der Klei, I.J., Kiel, J.A.K.W. & Veenhuis, M. (2001) Peroxisome biogenesis and selective degradation converge at Pex14p. *J. Biol. Chem.* **276**, 44570-44574.

15. van Zutphen, T., Veenhuis, M. & van der Klei, I.J. (2008) Pex14 is the sole component of the peroxisomal translocon that is required for pexophagy. *Autophagy* **4**, 63-66.

16. Iwata, J., Ezaki, J., Komatsu, M., Yokota, S., Ueno, T., Tanida, I., Chiba, T., Tanaka, K. & Kominami, E. (2006) Excess peroxisomes are degraded by autophagic machinery in mammals. *J. Biol. Chem.* **281**, 4035-4041.

17. Yamashita, S., Abe, K., Tatemichi, Y. & Fujiki, Y. (2014) The membrane peroxin PEX3 induces peroxisome-ubiquitination-linked pexophagy. *Autophagy* **10**, 1549-1564.

18. Deosaran, E., Larsen, K.B., Hua, R., Sargent, G., Wang, Y., Kim, S., Lamark, T., M. Jauregui, M., Law, K., Lippincott-Schwartz, J., Brech, A., Johansen, T. & Kim, P.K. (2013) NBR1 acts as an autophagy receptor for peroxisomes. *J. Cell. Sci.* **126**, 939-952.

19. Hara-Kuge, S. & Fujiki, Y. (2008) The peroxin Pex14p is involved in LC3-dependent degradation of mammalian peroxisomes. *Exp. Cell Res.* **314**, 3531-3541.

20. Ichimura, Y., Kirisako, T., Takao, T., Satomi, Y., Shimonishi, Y., Ishihara, N., Mizushima, N., Tanida, I., Kominami, E., Ohsumi, M., Noda, T. & Ohsumi, Y. (2000) A ubiquitin-like system mediates protein lipidation. *Nature* **408**, 488-492.

21. Sou, Y.S., Tanida, I., Komatsu, M., Ueno, T. & Kominami, E. (2006) Phosphatidylserine in addition to phosphatidylethanolamine is an *in vitro* target of the mammalian Atg8 modifiers, LC3, GABARAP, and GATE-16. *J. Biol. Chem.* **281**, 3017-3024.

22. Novak, I., Kirkin, V., McEwan, D.G., Zhang, J., Wild, P., Rozenknop, A., Rogov, V., Löhr, F., Popovic, D., Occhipinti, A., Reichert, A.S., Terzic, J., Dötsch, V.,

Ney, P.A. & Dikic, I. (2010) Nix is a selective autophagy receptor for mitochondrial clearance. *EMBO Rep.* **11**, 45-51.

23. Liu, L., Feng, D., Chen, G., Chen, M., Zheng, Q., Song, P., Ma, Q., Zhu, C., Wang, R., Qi, W., Huang, L., Xue, P., Li, B., Wang, X., Jin, H., Wang, J., Yang, F., Liu, P., Zhu, Y., Sui, S. & Chen, Q. (2012) Mitochondrial outer-membrane protein FUNDC1 mediates hypoxia-induced mitophagy in mammalian cells. *Nat. Cell Biol.* **14**, 177-185.

24. Pankiv, S., Clausen, T.H., Lamark, T., Brech, A., Bruun, J.A., Outzen, H., Øvervatn, A., Bjørkøy, G. & Johansen, T. (2007) p62/SQSTM1 binds directly to Atg8/LC3 to facilitate degradation of ubiquitinated protein aggregates by autophagy. *J. Biol. Chem.* **282**, 24131-24145.

25. Noda, N.N., Kumeta, H., Nakatogawa, H., Satoo, K., Adachi, W., Ishii, J., Fujioka, Y., Ohsumi, Y. & Inagaki, F. (2008) Structural basis of target recognition by Atg8/LC3 during selective autophagy. *Genes Cells* **13**, 1211-1218.

26. Gould, S.J., Keller, G.-A., Hosken, N., Wilkinson, J. & Subramani, S. (1989) A conserved tripeptide sorts proteins to peroxisomes. *J. Cell Biol.* **108**, 1657-1664.

27. Terlecky, S.R., Nuttley, W.M., McCollum, D., Sock, E. & Subramani, S. (1995) The *Pichia pastoris* peroxisomal protein PAS8p is the receptor for the C-terminal tripeptide peroxisome targeting signal. *EMBO J.* **14**, 3627-3634.

28. Wiemer, E.A., Nuttley, W.M., Bertolaet, B.L., Li, X., Francke, U., Wheelock, M.J., Anne, U.K., Johnson, K.R. & Subramani, S. (1995) Human peroxisomal targeting signal-1 receptor restores peroxisomal protein import in cells from patients with fatal peroxisomal disorders. *J. Cell Biol.* **130**, 51-65.

29. Itoh, R. & Fujiki, Y. (2006) Functional domains and dynamic assembly of the peroxin Pex14p, the entry site of matrix proteins. *J. Biol. Chem.* **281**, 10196-10205.

30. Kinoshita, N., Ghaedi, K., Shimozawa, N., Wanders, R.J.A., Matsuzono, Y., Imanaka, T., Okumoto, K., Suzuki, Y., Kondo, N. & Fujiki, Y. (1998) Newly identified Chinese hamster ovary cell mutants are defective in biogenesis of peroxisomal membrane vesicles (peroxisomal ghosts), representing a novel complementation group in mammals. *J. Biol. Chem.* **273**, 24122-24130.

31. Natsuyama, R., Okumoto, K. & Fujiki, Y. (2013) Pex5p stabilizes Pex14p: a study using a newly isolated *pex5* CHO cell mutant, ZPEG101. *Biochem. J.* **449**, 195-207.

32. Otera, H., Okumoto, K., Tateishi, K., Ikoma, Y., Matsuda, E., Nishimura, M., Tsukamoto, T., Osumi, T., Ohashi, K., Higuchi, O. & Fujiki, Y. (1998) Peroxisome targeting signal type 1 (PTS1) receptor is involved in import of both PTS1 and PTS2: Studies with *PEX5*-defective CHO cell mutants. *Mol. Cell. Biol.* **18**, 388-399.

33. Otera, H., Harano, T., Honsho, M., Ghaedi, K., Mukai, S., Tanaka, A., Kawai, A., Shimizu, N. & Fujiki, Y. (2000) The mammalian peroxin Pex5pL, the longer isoform of the mobile peroxisome targeting signal (PTS) type 1 transporter, translocates Pex7p-PTS2 protein complex into peroxisomes via its initial docking site, Pex14p. *J. Biol. Chem.* **275**, 21703-21714.

34. Shimizu, N., Itoh, R., Hirono, Y., Otera, H., Ghaedi, K., Tateishi, K., Tamura, S., Okumoto, K., Harano, T., Mukai, S. & Fujiki, Y. (1999) The peroxin Pex14p: cDNA cloning by functional complementation on a Chinese hamster ovary cell mutant, characterization, and functional analysis. *J. Biol. Chem.* **274**, 12593-12604.

35. Tsukamoto, T., Yokota, S. & Fujiki, Y. (1990) Isolation and characterization of Chinese hamster ovary cell mutants defective in assembly of peroxisomes. *J. Cell Biol.* **110**, 651-660.

36. Mukai, S., Ghaedi, K. & Fujiki, Y. (2002) Intracellular localization, function, and dysfunction of the peroxisome-targeting signal type 2 receptor, Pex7p, in mammalian cells. *J. Biol. Chem.* **277**, 9548-9561.

37. Otera, H., Setoguchi, K., Hamasaki, M., Kumashiro, T., Shimizu, N. & Fujiki, Y. (2002) Peroxisomal targeting signal receptor Pex5p interacts with cargoes and import machinery components in a spatiotemporally differentiated manner: conserved Pex5p WXXXF/Y motifs are critical for matrix protein import. *Mol. Cell. Biol.* **22**, 1639-1655.

38. Smith, D.B. & Johnson, K.S. (1988) Single-step purification of polypeptides expressed in *Escherichia coli* as fusions with glutathione *S*-transferase. *Gene.* **67**, 31-40.

39. Okumoto, K., Shimozawa, N., Kawai, A., Tamura, S., Tsukamoto, T., Osumi, T., Moser, H., Wanders, R.J.A., Suzuki, Y., Kondo, N. & Fujiki, Y. (1998) *PEX12*, the pathogenic gene of group III Zellweger syndrome: cDNA cloning by functional complementation on a CHO cell mutant, patient analysis, and characterization of Pex12p. *Mol. Cell. Biol.* **18**, 4324-4336.

40. Mizushima, N., Noda, T., Yoshimori, T., Tanaka, Y., Ishii, T., George, M.D.,

Klionsky, D.J., Ohsumi, M. & Ohsumi, Y. (1998) A protein conjugation system essential for autophagy. *Nature* **395**, 395-398.

41. Kabeya, Y., Mizushima, N., Ueno, T., Yamamoto, A., Kirisako, T., Noda, T., Kominami, E., Ohsumi, Y. & Yoshimori, T. (2000) LC3, a mammalian homologue of yeast Apg8p, is localized in autophagosome membranes after processing. *EMBO J.* **19**, 5720-5728.

42. Kirisako, T., Ichimura, Y., Okada, H., Kabeya, Y., Mizushima, N., Yoshimori, T., Ohsumi, M., Takao, T., Noda, T. & Ohsumi, Y. (2000) The reversible modification regulates the membrane-binding state of Apg8/Aut7 essential for autophagy and the cytoplasm to vacuole targeting pathway. *J. Cell Biol.* **151**, 263-276.

43. Oh-oka, K., Nakatogawa, H. & Ohsumi, Y. (2008) Physiological pH and acidic phospholipids contribute to substrate specificity in lipidation of Atg8. *J. Biol. Chem.* **283**, 21847-21852.

44. Wu, J., Dang, Y., Su, W., Liu, C., Ma, H., Shan, Y., Pei, Y., Wan, B., Guo, J. & Yu, L. (2006) Molecular cloning and characterization of rat *LC3A* and *LC3B*--Two novel markers of autophagosome. *Biochem. Biophys. Res. Commun.* **339**, 437-442.

45. Ichimura, Y., Kumanomidou, T., Sou, Y.S., Mizushima, T., Ezaki, J., Ueno, T., Kominami, E., Yamane, T., Tanaka, K. & Komatsu, M. (2008) Structural basis for sorting mechanism of p62 in selective autophagy. *J. Biol. Chem.* **283**, 22847-22857.

46. Su, J.R., Takeda, K., Tamura, S., Fujiki, Y. & Miki, K. (2009) Crystal structure of the conserved N-terminal domain of the peroxisomal matrix-protein-import receptor, Pex14p. *Proc. Natl. Acad. Sci. U. S. A.* **106**, 417-421.

47. Neufeld, C., Filipp F.V., Simon, B., Neuhaus, A., Schüller, N., David, C., Kooshapur, H., Madl, T., Erdmann, R., Schliebs, W., Wilmanns, M. & Sattler, M. (2009) Structural basis for competitive interactions of Pex14 with the import receptors Pex5 and Pex19. *EMBO J.* **28**, 745-754.

48. van der Leij, I., Franse, M.M., Elgersma, Y., Distel, B. & Tabak, H.F. (1993) PAS10 is a tetratricopeptide-repeat protein that is essential for the import of most matrix proteins into peroxisomes of *Saccharomyces cerevisiae*. *Proc. Natl. Acad. Sci. U. S. A.* **90**, 11782-11786.

49. Miyata, N. & Fujiki, Y. (2005) Shuttling mechanism of peroxisome targeting signal type 1 receptor Pex5: ATP-independent import and ATP-dependent export.

Mol. Cell. Biol. **25**, 10822-10832.

50. Rucktäschel, R., Girzalsky, W. & Erdmann, R. (2011) Protein import machineries of peroxisomes. *Biochim. Biophys. Acta* **1808**, 892-900.

51. Kiel, J.A.K.W., Komduur, J.A., van der Klei, I.J. & Veenhuis, M. (2003) Macropexophagy in *Hansenula polymorpha*: facts and views. *FEBS Lett.* **549**, 1-6.

52. Urquhart, A.J., Kennedy, D., Gould, S.J. & Crane, D.I. (2000) Interaction of Pex5p, the type 1 peroxisome targeting signal receptor, with the peroxisomal membrane proteins Pex14p and Pex13p. *J. Biol. Chem.* **275**, 4127-4136.

53. Oliveira, M.E.M., Reguenga, C., Gouveia, A.M.M., Guimaraes, C.P., Schliebs, W., Kunau, W.-H., Silvaa, M.T., Sa-Miranda, C. & Azevedo, J.E. (2002) Mammalian Pex14p: membrane topology and characterisation of the Pex14p–Pex14p interaction. *Biochim. Biophys. Acta* **1567**, 13-22.

54. Lamark, T., Kirkin, V., Dikic, I. & Johansen, T. (2009) NBR1 and p62 as cargo receptors for selective autophagy of ubiquitinated targets. *Cell Cycle* **8**, 1986-1990.

55. Mizushima, N., Levine, B., Cuervo, A.M. & Klionsky, D.J. (2008) Autophagy fights disease through cellular self-digestion. *Nature* **451**, 1069-1075.

56. Nordgren, M., Wang, B., Apanasets, O. & Fransen, M. (2013) Peroxisome degradation in mammals: mechanisms of action, recent advances, and perspectives. *Front. Physiol.* **4**, Article 145, doi: 10.3389/fphys.2013.00145.

FIGURE LEGENDS

Figure 1. Pex14p is important for binding to LC3 in autophagic degradation of peroxisomes upon starvation treatment.

(A) CHO-K1 cells were cultured under the normal or the starvation condition. Cell lysates were analyzed by immunoprecipitation using anti-Pex14p antibody conjugated to Protein A-Sepharose. Immunoprecipitates were assessed for Pex5p, Pex14p and LC3. Input, 5% of the lysates used for immunoprecipitation. The dot designates a suspected intermediate product of LC3-I converting to LC3-II, which has not been confirmed and could be non-specific. (B) Confocal microscopic images of CHO-K1 cells stably expressing EGFP-LC3B cultured under the normal (***C***) and starvation (***S***) conditions and re-culture after starvation (***SC***) in the absence or presence of Chloroquine. Colocalizations of EGFP-LC3-II and a lysosome marker, Lamp-1, with Pex14p were assessed. Scale bar, 10 μm.

Figure 2. LC3-II is synthesized *in vitro*.

(A) Purified recombinant human Atg proteins and mutant LC3 (LC3$_{TFG}$) were subjected to 15% SDS-PAGE and stained with Coomassie Brilliant Blue. (B) *In vitro* formation of hAtg7-LC3 (E1-substrate) intermediate. hAtg7 and LC3$_{TFG}$ were incubated in reconstitution buffer at 30°C for indicated time in the presence or absence of ATP and 100 mM DTT, as indicated at the top. Reaction mixture was subjected to SDS-PAGE under non-reducing condition. LC3-hAtg7 conjugate and LC3$_{TFG}$ were detected by immunoblotting using anti-LC3 antibody. (C) LC3-hAtg3 (E2-substrate) intermediate was synthesized *in vitro* as follows. hAtg7, hAtg3 and LC3$_{TFG}$ were mixed in reconstitution buffer and incubated at 30°C for 1 h in the presence or absence of ATP (lanes 2 and 3). Reaction was stopped by addition of an equal volume of SDS-PAGE sample buffer and the mixture was analyzed as in (B). Anti-LC3 antibody and anti-hAtg3 antibody were used for detection in immunoblotting assay. (D) LC3-II synthesis reaction was performed with different proportions of PE and PC, 7:3 or 5:5 respectively for indicated times. The reaction

mixture was analyzed as in (C). (E) hAtg7, hAtg3 and $LC3_{TFG}$ were mixed in reconstitution buffer and incubated at 30°C for 1 h in the presence of liposomes with the proportions of PE:PC=7:3. The reaction mixture was subjected to SDS-PAGE under non-reducing (lane 2) and denatured (lane 3) conditions respectively or centrifuged at 100,000 × *g* for 30 min. After centrifugation, supernatant (lane 4) and pellet (lane5) were also analyzed by SDS-PAGE and CBB staining. (F) Purified recombinant human Atg proteins and mutant LC3 ($LC3_{TFG}$) (0.1 μM each) in (A) were incubated at 30°C for 1 h with PE-containing liposomes (PE:PC=7:3) in reconstitution buffer in the presence (+) or absence (-) of ATP. Reaction mixtures were analyzed by SDS-PAGE and immunoblotting with anti-LC3 antibody.

Figure 3. Transmembrane domain of Pex14p is crucial for binding to LC3-II.

(A) Purified GST fusion proteins (upper panel) were immobilized to glutathione (GSH)-Sepharose and incubated at 4°C for 2 h with the reaction mixture of LC3-II conjugation system (see B) in the presence of 1% NP-40. GST and GST-p62 were also used as negative and positive controls, respectively. After the incubation, GSH-Sepharose was washed 3 times with reconstitution buffer. Proteins bound to GSH-Sepharose were analyzed by SDS-PAGE and immunoblotting with anti-LC3 antibody (lower panel). (B) Schematic diagram showing several domains in Pex14p and the constructed truncation mutants of Pex14p. Gray, orange, and pink regions represent the Pex5p-binding, transmembrane, and coiled-coil domains, respectively. (C) GST, GST-p62 and GST-fused full-length and deletion mutants of Pex14p were expressed and purified by GSH-Sepharose 4B (upper panel). Pull-down assay was performed as in Figure 1C, and proteins bound to GSH-Sepharose were analyzed by immunoblotting with anti-LC3 antibody (lower panel). The LC3-II bound to GST-fused proteins was quantified and represented with S.D. of four independent experiments. Each bar represents the ratio of LC3-II to respective GST-fused protein.

Figure 4. Pex5p inhibits the interaction between Pex14p and LC3-II.

(A) *pex14* ZP161 cells were cultured under the starvation condition. LC3 was purified

from the cytosolic and membrane fractions using anti-LC3 antibody conjugated to Protein A-Sepharose (lower panel, lanes 3 and 4). Recombinant His-Pex14p was incubated with the immobilized LC3 (lane 1). His-Pex14p bound to Protein A-Sepharose was detected by Western blotting with anti-His_6 tag antibody. Neg. represents a negative control without LC3 on the Sepharose (lane 2). (B) LC3-II was purified from the membrane fraction of *pex14* ZP161 cells cultured under the starvation condition and was immobilized with anti-LC3 antibody linked to Protein A-Sepharose. To the immobilized LC3 suspended in 300 µl 1% NP-40 lysis buffer, recombinant His-Pex14p was added with the indicated amounts of cytosol that had been prepared from the starved *pex5* ZPEG101 cells or wild-type CHO cells. His-Pex14p bound to Protein A-Sepharose was detected by Western blotting with anti-His_6 tag antibody. Input, 10% of the recombinant His-Pex14p used for binding assay. (C) In place of the cytosolic fraction, recombinant Pex5p or BSA as a control protein was added to the binding reaction. (D) CHO-K1 cells stably expressing EGFP-LC3B were grown on a cover-glass in F12/10% FCS medium (panels a-d and e-h). Recombinant His-Pex5pL was introduced into the cells using BioPORTER under the serum-free condition (panels i-l). After 4 h, the cells were permeabilized with 50 µg/ml digitonin, fixed with 4% PFA, and incubated with primary antibody to Pex14pC or His_6 tag and secondary antibody labeled with Alexa 568 or 647. Cells were monitored by a Carl-Zeiss confocal laser scan microscopy. Scale bar, 10 µm. (E) Recombinant His-Pex5pL and BSA were introduced into CHO-K1 cells stably expressing EGFP-LC3B using BioPORTER under the serum-free condition for 4 h. Cell lysates were analyzed by Western blotting with antibodies to His_6 tag, and α-tubulin, a loading control. (F) The percentage of EGFP-LC3-II positive peroxisomes was calculated. Data are presented as the mean ± S.D. of 3 replicates. (G) Recombinant His-Pex5pL and BSA were introduced into CHO-K1 cells stably expressing EGFP-LC3B using BioPORTER under the serum-free condition for 4 h, then re-cultured with normal culture medium for 2 h in the presence or absence of Chloroquine. Cell lysates were analyzed by Western blotting with antibodies to His_6 tag, Pex14p, AOx, tubulin and NBR1. Cell lysates were also analyzed by

immunoprecipitation using antibody to LC3. Immunoprecipitates were assessed for LC3 and NBR1.

Figure 5. Import defect caused by starvation initiates peroxisomal degradation. (A) Confocal microscopic images of CHO-K1 cells cultured under the normal (***C***) and starvation (***S***) conditions, respectively. Colocalizations with Pex14p of Pex5p (panels a-f) and PTS2 protein thiolase (panels g-l) were assessed. Scale bar, 10 μm. The percentages of Pex5p or thiolase positive peroxisomes were calculated. Data are presented as the mean ± S.D. of 3 replicates each. (B) The cytosol (cyt) and the membrane (mem) fractions were prepared from CHO-K1 and *pex5* ZP139 cells that had been cultured in F12/10% FCS (***C***) or starved in Hank's solution for 3 h (***S***) and were analyzed by immunoprecipitation using anti-LC3 antibody. Immunoprecipitates were assessed for Pex5p, Pex14p, and LC3. (C) Morphology of *EGFP-LC3B*-transfected CHO-K1 and ZP139 cells, both grown for 2 h under the nutrient-rich (***C***) (panels a-d and i-l) or the nutrient-starved (***S***) (panels e-h and m-p) conditions. Cells were stained with primary antibodies to Pex14p and Pex5p and secondary antibodies labeled with Alexa 568 and Alexa647, respectively. EGFP-LC3B was monitored by EGFP fluorescence. Scale bar, 10 μm. (D) The percentage of EGFP-LC3-II positive peroxisomes was calculated. Data are presented as the mean ± S.D. of 3 replicates. (E) Confocal microscopic images of ZP139 cells cultured under the normal (***C***) (panels a-c) and starved (***S***) (panels d-f) in Hank's solution for 5 h, respectively. Scale bar, 20 μm (panels a-c) and 10 μm (panels d-f). Pex5p in ZP139 cells was quantified after the culture in the normal medium for 2 h and starved in Hank's solution for 2, 4, and 6 h, respectively. LDH was used as an internal control. (F) Cell lysates from CHO-K1 and *pex5* ZP139 cells that had been cultured in F12/10% FCS (***C***) or starved in Hank's solution for 5 h (***S5***) in the presence of Bafilomycin A1 were analyzed by western blotting with antibodies to Pex5p, Pex14p and LC3. (G) GST-catalase was expressed in *E. coli*, purified with GSH-conjugated Sepharose 4B, and used for a pull-down assay. Cytosol fractions each from CHO-K1 cells cultured under the normal (***C***) and starvation (***S***) conditions

were subjected to a pull-down assay using the immobilized GST-catalase. Pex5p was detected by western blotting with anti-Pex5p antibody.

Figure 6. NBR1 is involved in the initiation of peroxisomal degradation.

(A) Coimmunoprecipitation assay was performed with antibodies to NBR1 and Flag using lysates from cultured (***C***) or starved (***S***) cells. Immunoprecipitates were assessed for NBR1, Pex14p, p62 and LC3 with respective specific antibodies. Input, 5% of the fractions used for immunoprecipitation. (B) Morphology of *EGFP-LC3B*-transfected CHO-K1 cells grown for 2 h under the conditions of normal (***C***) (panels a-d) and starvation (***S***) (panels e-h). NBR1 was knocked down in CHO-K1 cells by transfecting *NBR1 siRNA* at a final concentration of 100 nM for 48 h. The cells were then starved for 2 h (panels i-l). Cells were stained with primary antibodies to Pex14p and NBR1 and secondary antibodies labeled with Alexa 568 and Alexa 647, respectively. EGFP-LC3B was monitored by EGFP fluorescence. Scale bar, 10 μm. (C) The percentage of EGFP-LC3-II positive peroxisomes was calculated. Data are presented as the mean ± S.D. of 3 replicates.

Acknowledgments

First of all, I would like to express my gratitude to all those who helped me during the thesis work.

My deepest gratitude goes first and foremost to Prof. Y. Fujiki, my supervisor, for his constant encouragement and guidance in the academic studies. High tribute shall be paid to Dr. S. Kuge and Dr. S. Yamashita for their instructive advices and suggestions in the completion of this thesis. I am particularly grateful to Prof. S. Tamura for his careful and patient guidance on my studying. I also would like to express my regards to Dr. K. Okumoto, Dr. M. Honsho, Dr. H. Niwa and Dr. S. Mukai for providing me with inspiring advice. Last but not the least, my thanks extend to all the members in the lab, who support me a lot not only as technical co-workers but also generous friends.

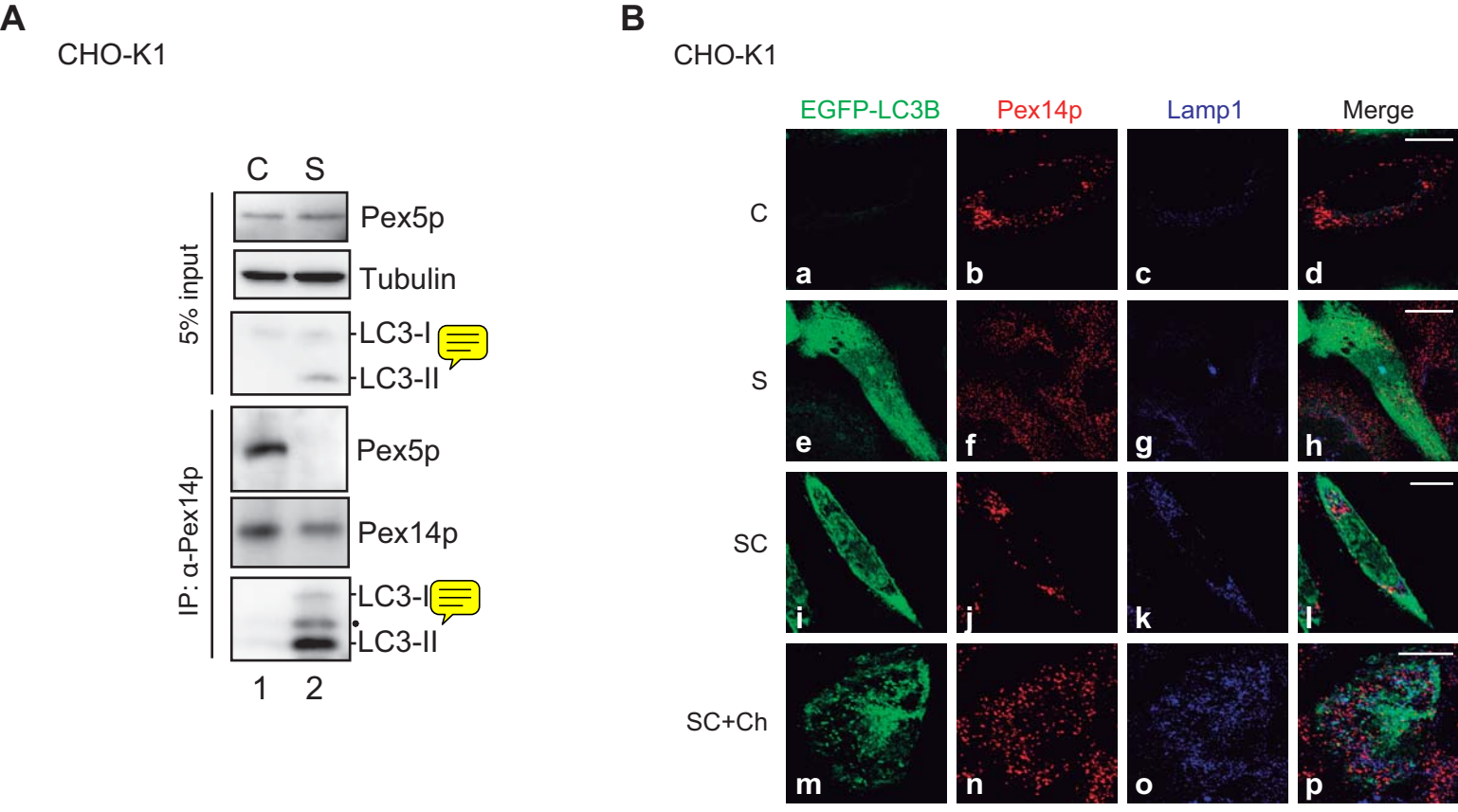
A
CHO-K1
C
S
5% input
Pex5p
Tubulin
LC3-I
LC3-II
IP: α-Pex14p
Pex5p
Pex14p
LC3-I
LC3-II
1
2
B
CHO-K1
EGFP-LC3B
Pex14p
Lamp1
Merge
C
S
SC
SC+Ch
a
b
c
d
e
f
g
h
i
j
k
l
m
n
o
p

Fig. 1

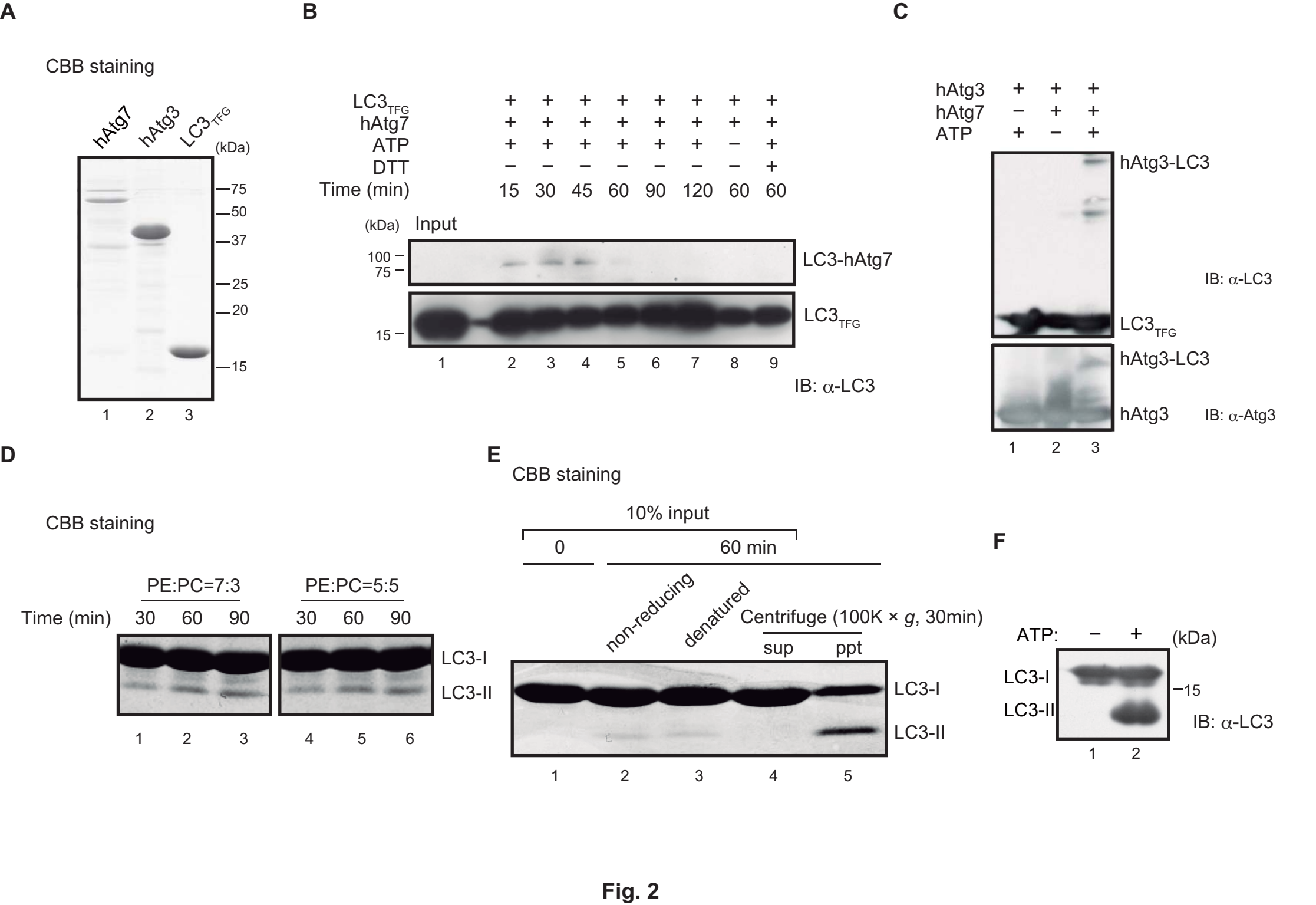
A
CBB staining
hAtg7
hAtg3
LC3TFG
(kDa)
75
50
37
25
20
15
1 2 3
B
LC3TFG + + + + + + + +
hAtg7 + + + + + + + +
ATP + + + + + + − +
DTT − − − − − − − +
Time (min) 15 30 45 60 90 120 60 60
(kDa) Input
100
75
15
LC3-hAtg7
LC3TFG
1 2 3 4 5 6 7 8 9
IB: α-LC3
C
hAtg3 + + +
hAtg7 − + +
ATP + − +
hAtg3-LC3
LC3TFG
IB: α-LC3
hAtg3-LC3
hAtg3
IB: α-Atg3
1 2 3
D
CBB staining
PE:PC=7:3
PE:PC=5:5
Time (min) 30 60 90 30 60 90
LC3-I
LC3-II
1 2 3 4 5 6
E
CBB staining
10% input
0
60 min
non-reducing
denatured
Centrifuge (100K × g, 30min)
sup
ppt
LC3-I
LC3-II
1 2 3 4 5
F
ATP: − +
(kDa)
LC3-I
LC3-II
15
IB: α-LC3
1 2

Fig. 2

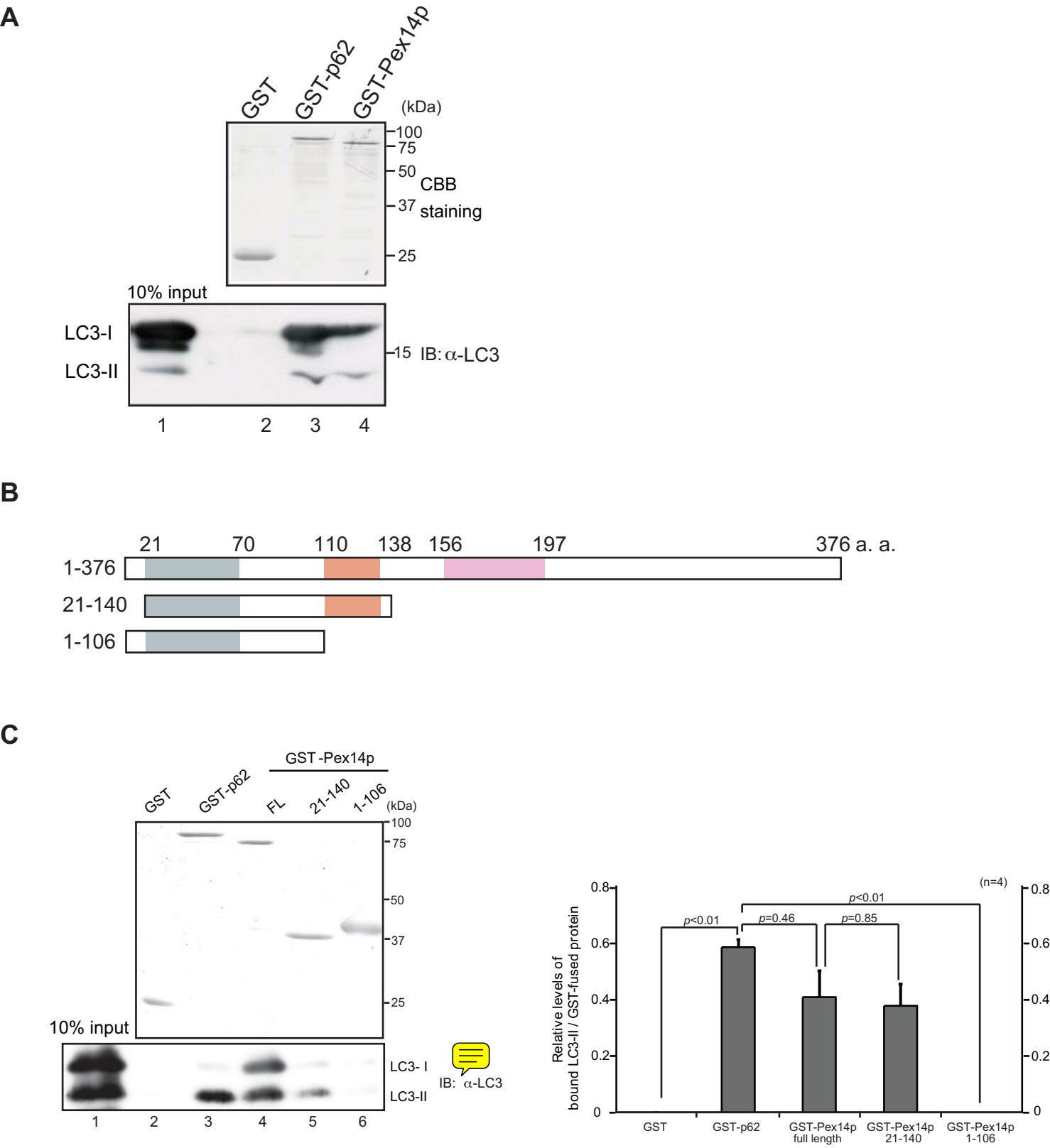
A
GST
GST-p62
GST-Pex14p
(kDa)
100
75
50
37
25
CBB staining
10% input
LC3-I
LC3-II
15
IB: α-LC3
1
2
3
4
B
21
70
110
138
156
197
376 a. a.
1-376
21-140
1-106
C
GST-Pex14p
GST
GST-p62
FL
21-140
1-106
(kDa)
100
75
50
37
25
10% input
LC3- I
LC3-II
IB: α-LC3
1
2
3
4
5
6
(n=4)
p<0.01
p=0.46
p=0.85
p<0.01
Relative levels of bound LC3-II / GST-fused protein
0.8
0.6
0.4
0.2
0
GST
GST-p62
GST-Pex14p full length
GST-Pex14p 21-140
GST-Pex14p 1-106

Fig. 3

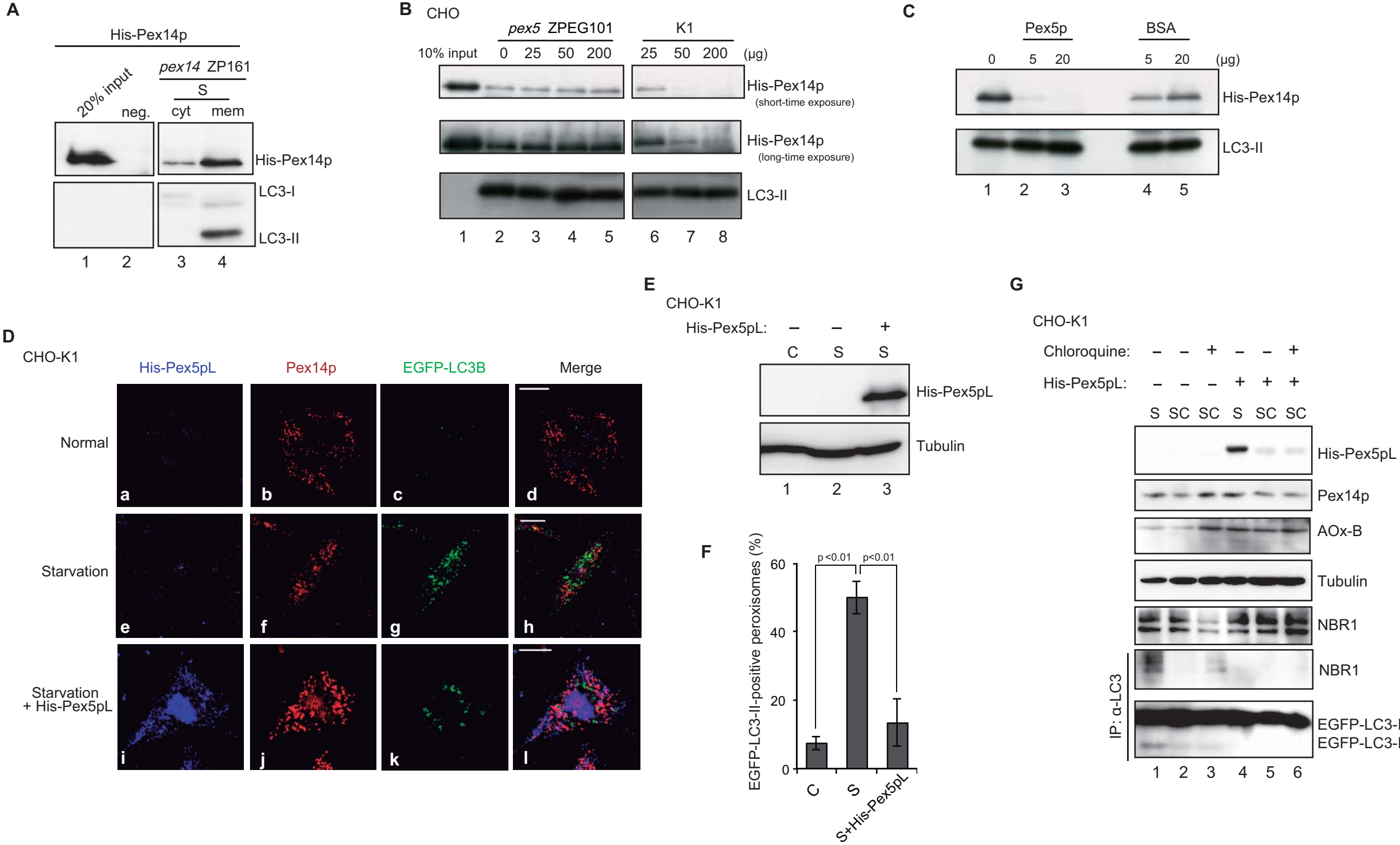
A
His-Pex14p
20% input
pex14 ZP161
S
neg.
cyt
mem
His-Pex14p
LC3-I
LC3-II
1 2 3 4
B
CHO
pex5 ZPEG101
K1
10% input
0 25 50 200
25 50 200 (μg)
His-Pex14p
(short-time exposure)
His-Pex14p
(long-time exposure)
LC3-II
1 2 3 4 5 6 7 8
C
Pex5p
BSA
0 5 20
5 20 (μg)
His-Pex14p
LC3-II
1 2 3 4 5
D
CHO-K1
His-Pex5pL
Pex14p
EGFP-LC3B
Merge
Normal
Starvation
Starvation
+ His-Pex5pL
a b c d
e f g h
i j k l
E
CHO-K1
His-Pex5pL: – – +
C S S
His-Pex5pL
Tubulin
1 2 3
F
EGFP-LC3-II-positive peroxisomes (%)
p<0.01 p<0.01
60
40
20
0
C
S
S+His-Pex5pL
G
CHO-K1
Chloroquine: – – + – – +
His-Pex5pL: – – – + + +
S SC SC S SC SC
His-Pex5pL
Pex14p
AOx-B
Tubulin
NBR1
NBR1
IP: α-LC3
EGFP-LC3-I
EGFP-LC3-II
1 2 3 4 5 6

Fig. 4

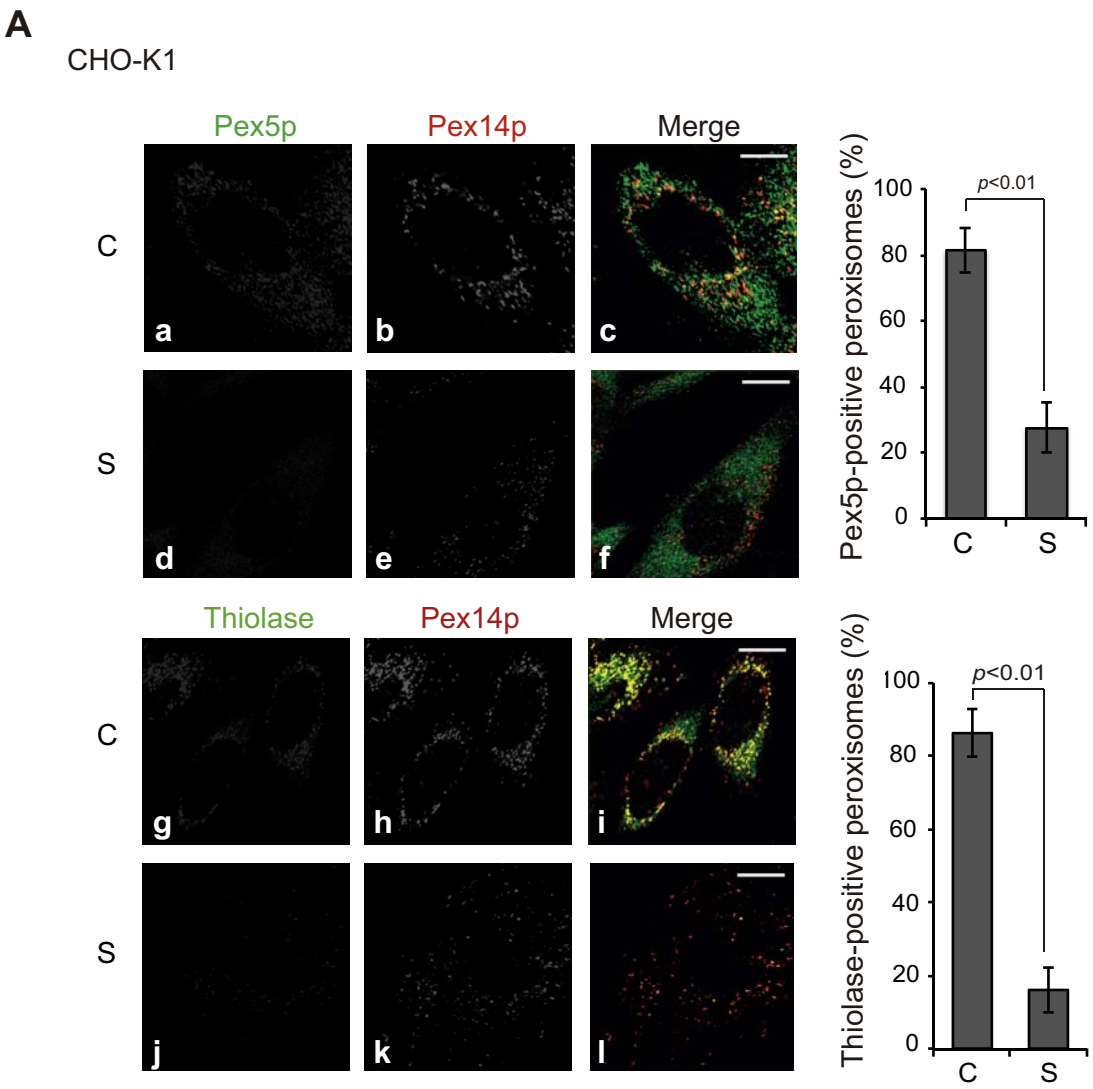
A
CHO-K1
Pex5p
Pex14p
Merge
C
S
a
b
c
d
e
f
Pex5p-positive peroxisomes (%)
p<0.01
100
80
60
40
20
0
C
S
Thiolase
Pex14p
Merge
g
h
i
j
k
l
Thiolase-positive peroxisomes (%)
p<0.01

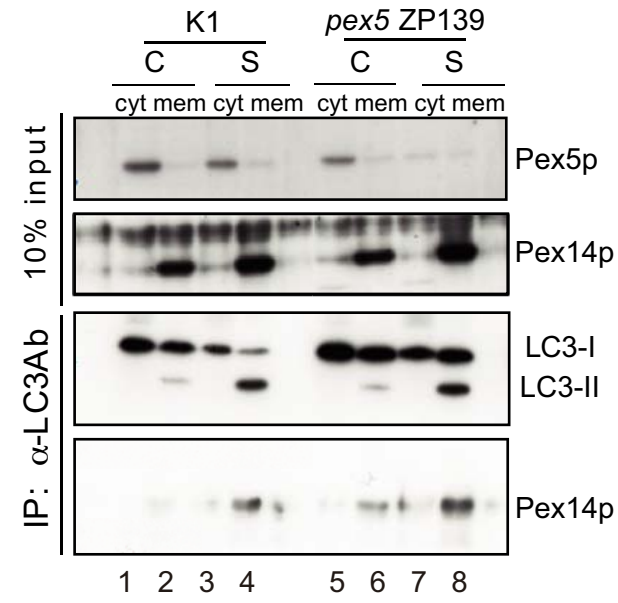
B
CHO
K1
pex5 ZP139
C
S
cyt mem cyt mem cyt mem cyt mem
10% input
Pex5p
Pex14p
IP: α-LC3Ab
LC3-I
LC3-II
Pex14p
1 2 3 4 5 6 7 8

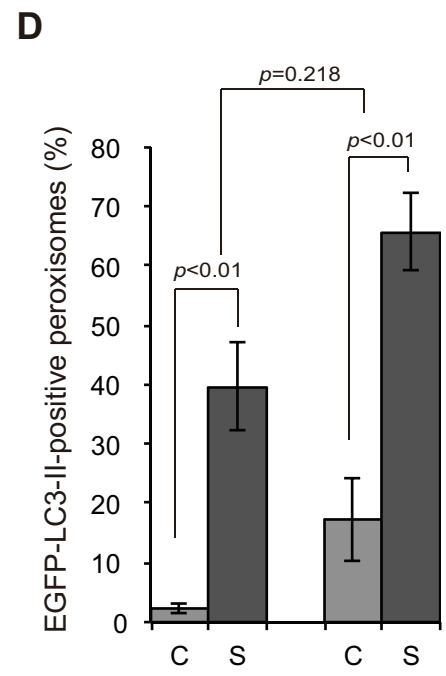
D
p=0.218
p<0.01
p<0.01
EGFP-LC3-II-positive peroxisomes (%)
80
70
60
50
40
30
20
10
0
C
S
C
S

C
CHO
Pex5p
Pex14p
EGPF-LC3B
Merge
K1
pex5 ZP139
C
S
a
b
c
d
e
f
g
h
i
j
k
l
m
n
o
p

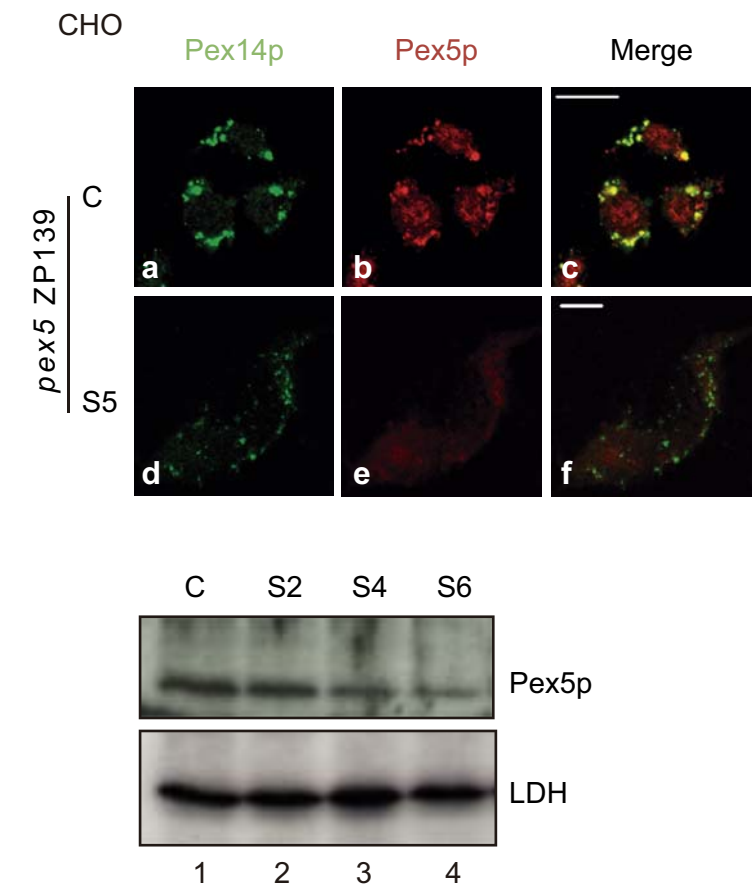
E
CHO
Pex14p
Pex5p
Merge
pex5 ZP139
C
S5
a
b
c
d
e
f
C
S2
S4
S6
Pex5p
LDH
1 2 3 4

F
CHO
K1
pex5 ZP139
C
S5
C
S5
Bafilomycin A1:
–
+
–
+
Pex5p
Pex14p
LC3-I
LC3-II
1 2 3 4

G
CHO-K1
Input (20%)
GST-catalase
GST
C
S
C
S
C
S
Pex5p
1 2 3 4 5 6

Fig. 5

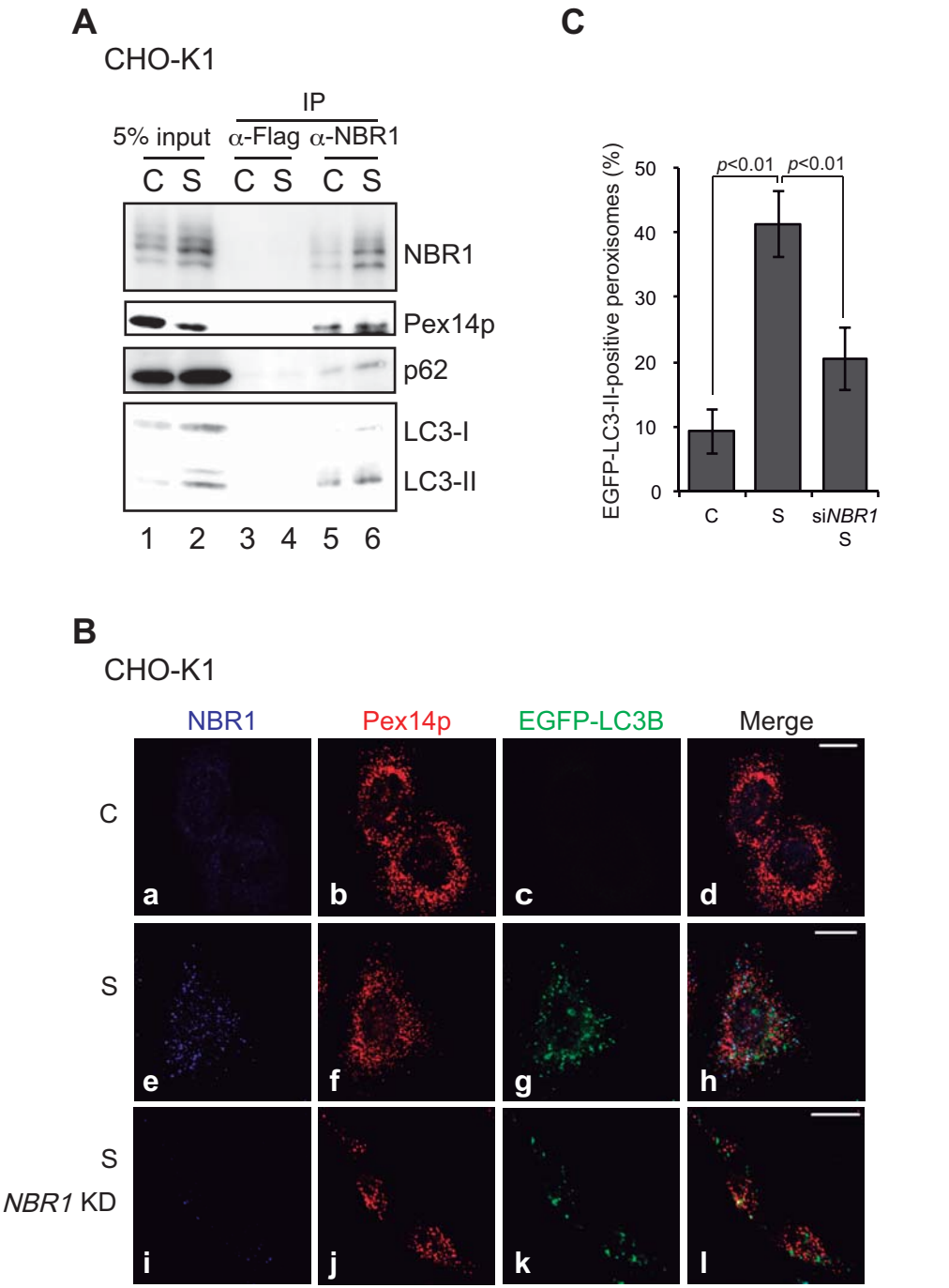
A
CHO-K1
IP
5% input
α-Flag
α-NBR1
C S C S C S
NBR1
Pex14p
p62
LC3-I
LC3-II
1 2 3 4 5 6
C
p<0.01
p<0.01
EGFP-LC3-II-positive peroxisomes (%)
50
40
30
20
10
0
C
S
siNBR1 S
B
CHO-K1
NBR1
Pex14p
EGFP-LC3B
Merge
C
S
S
NBR1 KD
a
b
c
d
e
f
g
h
i
j
k
l

Fig. 6